

# Low-Loss Rectangular Dielectric Image Line for Millimeter-Wave Integrated Circuits

SHUICHI SHINDO AND TAKAO ITANAMI

**Abstract**—This paper describes some fundamental properties of a low-loss  $E_{11}^x$  mode rectangular dielectric image line where the electric field is parallel to the metal image plane. This image line is characterized by its low transmission loss, compared with the conventional dominant  $E_{11}^y$  mode rectangular dielectric image line. The transmission loss of this new image line is nearly less than half that of the  $E_{11}^y$  mode rectangular dielectric image line. As an application example, a bandpass filter is developed using this  $E_{11}^x$  mode rectangular dielectric image line and the measurement results of its frequency responses in the 50-GHz range are presented. Although the  $E_{11}^x$  mode is a higher order mode in the rectangular dielectric image line, reasonable bandpass filter characteristics have been realized.

the electric field is parallel to the metal image plane. The  $E_{11}^x$  mode rectangular dielectric image line transmission loss is calculated, measured, and compared with that of the dominant  $E_{11}^y$  mode rectangular dielectric image line. As the  $E_{11}^x$  mode is a higher order mode in the rectangular dielectric image line, spurious modes occur in curved image line devices, such as couplers and resonators. A bandpass filter, that is composed of the  $E_{11}^x$  mode rectangular dielectric image lines and two pillbox resonators, is fabricated and its frequency response in the 50-GHz range is measured.

## I. INTRODUCTION

THE DIELECTRIC image line has received renewed interest in recent years for millimeter-wave integrated circuits. A number of passive and active millimeter-wave devices have been investigated in dielectric image line technologies [1]. The reason for this interest is that, in the regions from millimeter wave to optical waves, the metal wall structures cause attenuation due to skin effect loss. This conduction loss is proportional to the square root of the frequency. Since the dielectric image line is not enclosed by the metal wall, the conduction loss is caused by only one metal image plane. This metal plane may also provide a heat sink and is convenient for dc biasing of integrated circuit devices.

Another source of attenuation is absorption due to the dielectric material. This dielectric loss depends on the  $\tan \delta$  and the dimension of the dielectric material. In practice, however, the cross-sectional dimensions of the dielectric become rather large in order to confine most of the energy within the dielectric.

Recently, a decrease in rectangular dielectric image line conduction loss has been achieved by the insular line [2], which has another thin dielectric between the rectangular dielectric core and the metal image plane. In the insular line the conduction loss is typically less than half that of the rectangular dielectric image line. Further, in the inverted strip dielectric waveguide [3] conduction loss is small, since most of the energy is in the guiding layers, separated from the metal plane.

In this work, another scheme to reduce rectangular dielectric image line conduction loss is proposed by using the  $E_{11}^x$  mode in a rectangular dielectric image line, where

## II. THEORETICAL CONSIDERATIONS

The rectangular dielectric image line, as depicted in Fig. 1, consists of a rectangular dielectric core with relative dielectric constant  $\epsilon_r$  surrounded by semi-infinite medium of dielectric constant  $\epsilon_0$  (usually air) and the metal image plane attached to the dielectric core. This image line can support a discrete spectrum of guided modes  $E_{mn}^x$  and  $E_{mn}^y$  ( $m = 1, 2, 3, \dots, n = 1, 3, 5, \dots$ ), and also a continuous spectrum of unguided modes. Subindices  $m$  and  $n$  indicate the number of half cycle variations each component has within the dielectric core. The main transverse field components of the  $E_{mn}^x$  modes are  $E_x$  and  $H_y$ , whereas those of the  $E_{mn}^y$  mode are  $E_y$  and  $H_x$ . The dominant mode is the  $E_{11}^y$  mode, as shown in Fig. 2(a), whose field variation is given by a cosine function, which outside the dielectric core (on top and on both sides) decays exponentially. The  $E_{11}^x$  mode shown in Fig. 2(b), that is called the  $E_{12}^x$  mode in the rectangular dielectric waveguide in free space, is a higher order mode and is orthogonally polarized with respect to the  $E_{11}^y$  mode. The  $E_{11}^x$  mode of the image line is the lowest mode in the  $E_{mn}^x$  modes and is launched as easily as the  $E_{11}^y$  mode. The  $y$  direction field variation is given by a sine function, because of the metal image plane.

A theoretical analysis of rectangular dielectric image line propagation characteristics was initially described by Toulios and Knox [4]. Dispersion curves, giving the ratio of free space wavelength  $\lambda_0$  to the guide wavelength  $\lambda_g$ , are shown in Fig. 3. The guide wavelength is dependent on the normalized guide dimension, defined as

$$B = \frac{4b}{\lambda_0} \sqrt{\epsilon_r - 1} . \quad (1)$$

The guide wavelength in Fig. 3 has been determined for a teflon core ( $\epsilon_r = 2.0$ ) having a  $2a \times b$  cross section, where  $a/b = 1$ . This cross section, in which the dielectric core

Manuscript received October 7, 1977.

The authors are with Yokosuka Electrical Communication Laboratory, NTT, Yokosuka-shi, 238-03 Japan.

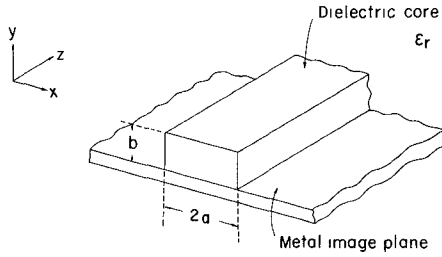


Fig. 1. Rectangular dielectric image line.

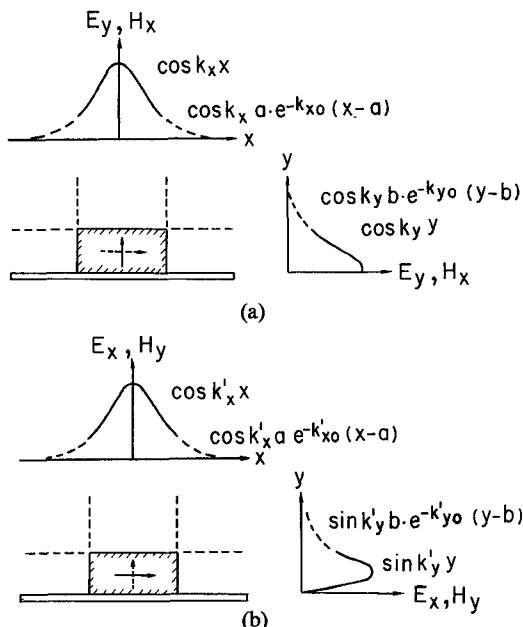
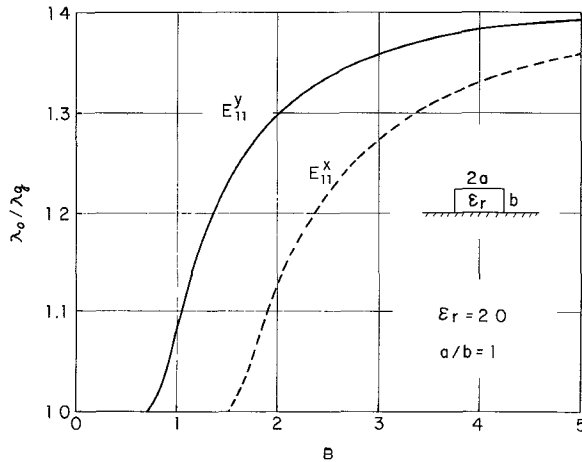
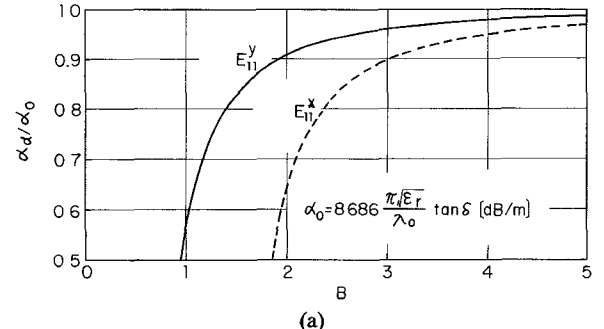


Fig. 2. Rectangular dielectric image line field distribution.

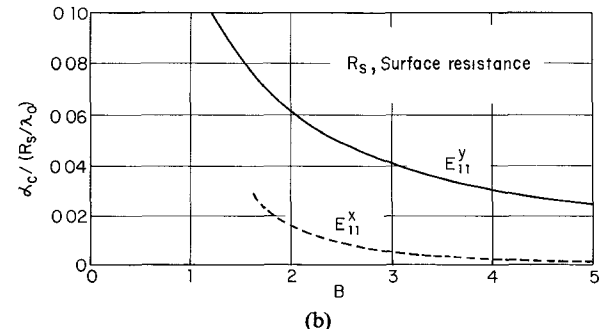
Fig. 3. Dispersion curves for  $E_{11}^y$  mode and  $E_{11}^x$  mode.

width is double its height, is equivalent to a rectangular dielectric waveguide in free space with aspect ratio  $a/b = 1$ .

The  $E_{11}^y$  mode rectangular dielectric image line attenuation constant, that consists of dielectric loss  $\alpha_d$  and conduction loss  $\alpha_c$ , has already been calculated [5]. By introducing a complex dielectric constant to allow for small losses in the dielectric core, the characteristic equations



(a)



(b)

Fig. 4. Calculated attenuation constant for  $E_{11}^y$  mode and  $E_{11}^x$  mode.

tions can be expanded in a Taylor series form, using solutions of the characteristic equation for a loss-less dielectric to determine the point about which the expansion is made. The first-order terms in the expansion can be used to derive an approximate expression for dielectric loss  $\alpha_d$  due to  $\tan \delta$ . The conduction loss  $\alpha_c$  analysis method is similar to that used in calculating the loss in ordinary metallic waveguides. In this approach, it is assumed that finite guide wall conductivity will have only a small effect on field configurations. In particular, the magnetic field tangential to the wall is expected to depend only slightly on the conductivity of the wall. This is very nearly true, as long as the conductivity is high, as it is for most metals. Conduction loss  $\alpha_c$  is given by

$$\alpha_c = \frac{W_1}{2W_t} \quad (2)$$

where  $W_1$  is lost power per unit length and  $W_t$  is transmitted power.

The above mentioned method can be applied to determine the  $E_{11}^x$  mode rectangular dielectric image line attenuation constant. The ratio of dielectric loss  $\alpha_d$  to the infinite dielectric medium attenuation constant  $\alpha_0$ ,

$$\alpha_0 = 8.686 \frac{\pi \sqrt{\epsilon_r}}{\lambda_0} \tan \delta \quad [\text{dB/m}] \quad (3)$$

is shown in Fig. 4(a), and conduction loss  $\alpha_c$  that is normalized to  $R_s/\lambda_0$  ( $R_s$  is surface resistance), is shown in Fig. 4(b), for the same rectangular dielectric image line as shown in Fig. 3.

$\alpha_d/\alpha_0$  approaches unity with increasing normalized guide dimension  $B$ , because of greater field confinement in the dielectric core. As the  $E_{11}^x$  mode field confinement is less than that of the  $E_{11}^y$  mode, even if  $B$  is the same

value, the  $E_{11}^x$  mode dielectric loss is less than that of the  $E_{11}^y$  mode. On the other hand, conduction loss  $\alpha_c$  decreases with increasing normalized guide dimension  $B$ , because the energy is mainly confined to the dielectric core and the influence of the metal image plane disappears.  $W_1$  and  $W_t$  in (2) are expressed as

$$W_1 = \frac{R_s}{2} \int \int \mathbb{H}_{\tan} \cdot \mathbb{H}_{\tan} da \quad (4)$$

$$W_t = \frac{Z_s}{2} \int \int \mathbb{H}_t \cdot \mathbb{H}_t da \quad (5)$$

where  $\mathbb{H}_{\tan}$  is the tangential magnetic field on the metal surface,  $\mathbb{H}_t$  is the transverse magnetic field, and  $Z_s$  is the wave impedance in the propagation direction. The integration in (4) and (5) is taken over the metal surface of a unit length and the cross-section area of the image line, respectively.  $\mathbb{H}_{\tan}$  of the  $E_{11}^y$  mode contains  $H_x$  and  $H_z$ , but that of the  $E_{11}^x$  mode contains only  $H_z$ . Therefore, the conduction loss is less than one-tenth that of the  $E_{11}^y$  mode. The above discussions neglect losses due to adhesives or metal surface roughness, which would increase overall image line attenuation.

### III. EXPERIMENTAL STUDIES

Rectangular dielectric image lines were fabricated and experiments were carried out in the 50-GHz range. The dielectric core was teflon ( $\epsilon_r = 2.0$ ), 3 mm high and 6 mm wide, and it was kept down on a silver-plated image plane by the foam dielectric slab. The normalized guide dimension  $B$  at 50 GHz in which the  $E_{11}^y$  mode and the  $E_{11}^x$  mode are the guided modes is 2.0.

The attenuation constant was measured from 50–54 GHz. Results are shown in Fig. 5, with the calculated attenuation constants. Measurements were accomplished by the transmission technique, where power was launched from a conventional wave guide, using a rectangular horn, and the power at the far end was measured by a similar horn. A small amount of power was radiated from the transmitting horn. However, in practice, this was found to be negligible compared with the power traveling down the image line. Excluding the launching losses at both transmitting and receiving horns, by measuring the transmission losses of different length image lines, an attenuation constant was obtained.

The theoretical attenuation constants are shown in Figs. 4(a) and (b) and in Table I at 50 GHz, where the teflon  $\tan \delta$  is  $1.5 \times 10^{-4}$  and the silver conductivity is  $6.17 \times 10^7 \text{ S/m}$ . The agreement between the theoretical and the experimental results is not always as good as shown in Fig. 5, which may be caused by the adhesives between the dielectric core and the metal plane, and by the measurement accuracy. The  $E_{11}^x$  mode rectangular dielectric image line attenuation constant is explicitly much less than that of the  $E_{11}^y$  mode rectangular dielectric image line.

Curved sections of the rectangular dielectric image line also suffer from radiation loss [6], which depends on the bending radius of a curved section and also depends on

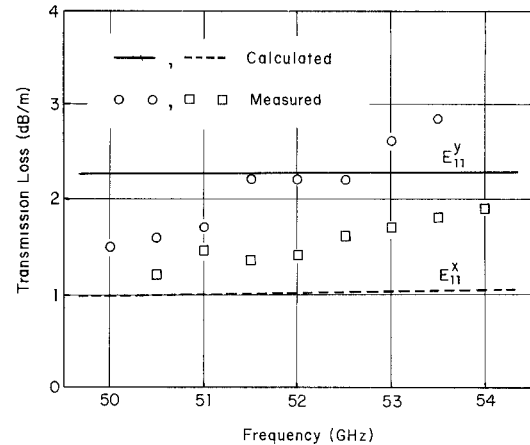


Fig. 5. Rectangular dielectric image line transmission loss ( $\epsilon_r = 2.0$ ,  $a/b = 1$ ).

TABLE I

Attenuation	$E_{11}^y$ mode	$E_{11}^x$ mode
* Dielectric Loss	0.87 dB/m	0.63 dB/m
** Conduction Loss	1.39	0.36
Total	2.26	0.99

\*  $\epsilon_r = 2.0$ ,  $\tan \delta = 1.5 \times 10^{-4}$

\*\* conductivity  $\sigma = 6.17 \times 10^7 \text{ S/m}$

the dielectric constant and the cross-sectional dimensions used. Another disadvantage of curved sections of the rectangular dielectric image line is the coupling to higher order modes. This increases the radiation losses, if the higher order modes are unguided modes. Unfortunately, there is little quantitative data available on the rectangular dielectric image line, especially on the  $E_{11}^x$  mode rectangular dielectric image line. In this work, experimental investigations were accomplished to distinguish radiation losses between  $E_{11}^y$  mode and  $E_{11}^x$  mode.

Fig. 6 shows the  $E_{11}^y$  mode and  $E_{11}^x$  mode teflon image line radiation losses. Cross-sectional dimensions are the same as shown in Fig. 5. Bending radius is 30 mm. In the 50–54-GHz range, the  $E_{11}^y$  mode radiation loss decreased from 0.43 dB/rad–0.12 dB/rad, and that of the  $E_{11}^x$  mode decreased from 0.75–0.50 dB/rad, with increasing frequency. The  $E_{11}^x$  mode radiation loss was much greater than that of the  $E_{11}^y$  mode, because the  $E_{11}^x$  mode field confinement is less than that of the  $E_{11}^y$  mode in the same normalized guide dimension  $B$ , where much energy is radiated from the curved sections. In order to confine the  $E_{11}^x$  mode field, the normalized guide dimension  $B$  is increased, namely the dielectric constant or the dielectrical core dimension is increased for a given frequency. Another method of decreasing radiation loss is to increase the aspect ratio  $a/b$ . The radiation loss of the  $E_{12}^x$  mode rectangular dielectric waveguide in free space with  $a/b = 2$  is almost the same as that of the  $E_{11}^y$  mode rectangular

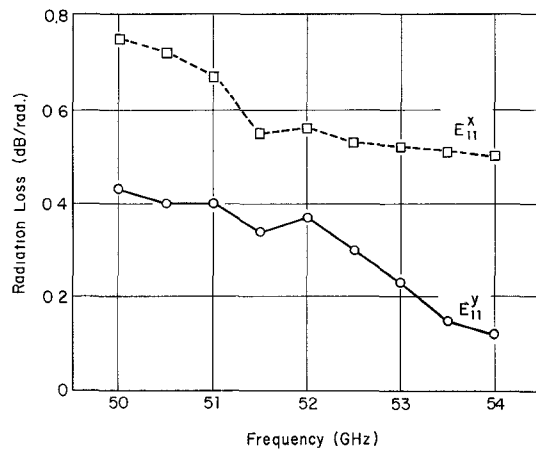


Fig. 6. Radiation loss in rectangular dielectric image line having a 30-mm curved radius.

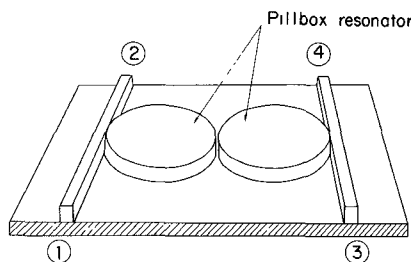


Fig. 7. Bandpass filter with two pillbox resonators.

dielectric waveguide in free space with  $a/b=1$ , according to the calculation of [7]. The  $E_{12}^x$  mode in the rectangular dielectric waveguide in free space is equivalent to the  $E_{11}^x$  mode in the rectangular dielectric image line, consequently the radiation loss of the  $E_{11}^x$  mode in image line can be decreased.

#### IV. CHARACTERISTICS OF A BANDPASS FILTER

As the  $E_{11}^x$  mode, previously mentioned, is a higher order mode in the rectangular dielectric image line, bends and couplers will cause coupling of the spurious modes. This increases loss in passive and active devices for the millimeter-wave integrated circuits, and also causes ripples in frequency responses. Therefore, to investigate these characteristics, a bandpass filter using the  $E_{11}^x$  mode rectangular dielectric image line was fabricated and its frequency response was measured.

The bandpass filter consists of two pillbox resonators, as shown in Fig. 7. Fused quartz ( $\epsilon_r=3.8$ ) was used to realize the small-sized filter. A disadvantage, for some applications, of this type of filter is the fact that multiple bandpass responses occur. The separation of spurious responses from a desired response is a function of the radius of the resonator. Increased separation can be obtained through a radius reduction, but at the expense of radiation loss from the resonator. For a given radius of the resonator, the radiation loss of the pillbox resonator is less than that of the ring resonator [8]. In Fig. 7, the aspect ratio of the input and output straight image line is 0.25 ( $a=1$  mm and  $b=4$  mm), in order to obtain

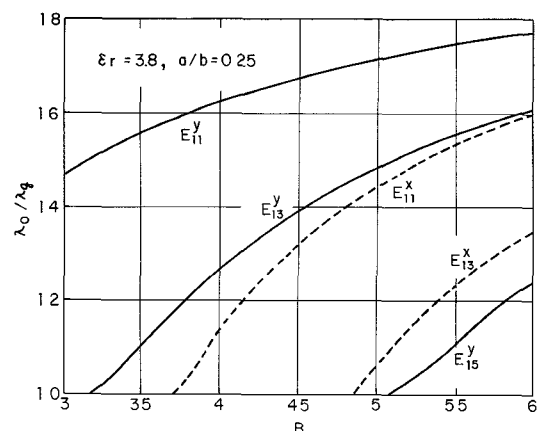


Fig. 8. Rectangular dielectric image line dispersion curves for  $\epsilon_r=3.8$  and  $a/b=0.25$ .

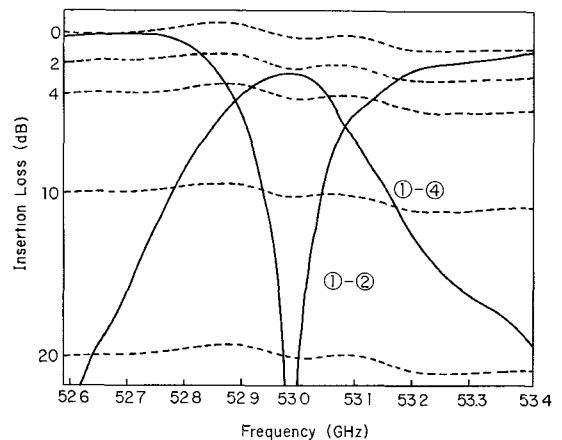


Fig. 9. Measured frequency responses of bandpass filter.

sufficient coupling to the pillbox resonators. The separation between two pillbox resonators is about 1 mm, and each pillbox resonator is in contact with the adjacent straight image line. The dispersion curves of this image line are shown in Fig. 8. The  $E_{11}^y$  mode and  $E_{13}^y$  mode are lower order modes than the  $E_{11}^x$  mode, but the degenerate mode to the  $E_{11}^x$  mode does not exist. The radius of the pillbox resonators is selected as 10 mm, to separate the adjacent spurious responses by about ten times the passband width (200 MHz).

The measured frequency response of the bandpass filter is shown in Fig. 9, the center frequency was 52.99 GHz, and the insertion loss was 2.2 dB. Adjacent spurious responses occurred at about 50.5 and 55.6 GHz, which agreed with the predictions. The bandpass filter was found to have reasonable characteristics, except for the insertion loss. The large insertion loss is due to the low  $Q$  of the resonator, mainly due to radiation from the curved surface. It is necessary to investigate the radiation phenomena, to possibly reduce radiation loss, by a better choice of the dielectric and the structure.

#### V. CONCLUSION

Some fundamental properties of the low-loss  $E_{11}^x$  mode rectangular dielectric image line have been discussed both

theoretically and experimentally, compared with the dominant  $E_{11}^y$  mode rectangular dielectric image line. The  $E_{11}^x$  mode attenuation constant was found to be nearly half that of the  $E_{11}^y$  mode in the 50-GHz range.

A bandpass filter, using the  $E_{11}^x$  mode rectangular dielectric image line, was fabricated and measured. Its frequency response was found to have reasonable characteristics, although radiation loss limited the achievable insertion loss. This image line device is believed to be useful for millimeter-wave integrated circuit applications.

#### ACKNOWLEDGMENT

The authors wish to thank M. Shinji and Dr. I. Ohtomo, of the Yokosuka Electrical Communication Laboratory, Nippon Telegraph and Telephone Public Corporation, for their valuable discussions and encouragement.

#### REFERENCES

- [1] R. M. Knox, "Dielectric waveguide microwave integrated circuits—An overview," *IEEE Trans. Microwave Theory Tech.*, vol. MTT-24, pp. 806–814, Nov. 1976.
- [2] ———, "Dielectric waveguide: A low-cost option for ICs," *Micro-waves*, pp. 56–67, Mar. 1976.
- [3] T. Itoh, "Inverted strip dielectric waveguide for millimeter-wave integrated circuits," *IEEE Trans. Microwave Theory Tech.*, vol. MTT-24, pp. 821–827, Nov. 1976.
- [4] R. M. Knox and P. P. Toullos, "Integrated circuits for the millimeter through optical frequency range," presented at *Proc. of the Symp. Submillimeter Waves*, New York, NY, Mar. 1970.
- [5] P. P. Toullos and R. M. Knox, "Rectangular dielectric image lines for millimeter integrated circuits," presented at *Western Electronics Show and Convention*, Los Angeles, CA, Aug. 1970.
- [6] R. M. Knox, P. P. Toullos, and J. Q. Howell, "Radiation losses in curved dielectric image waveguides of rectangular cross section," presented at *IEEE MTT-S Int. Microwave Symp.*, Boulder, CO, June 1973.
- [7] E. A. J. Marcatili and S. E. Miller, "Improved relations describing directional control in electromagnetic wave guidance," *Bell Syst. Tech. J.*, vol. 48, pp. 2161–2188, Sept. 1969.
- [8] E. A. J. Marcatili, "Bends in optical dielectric guides," *Bell Syst. Tech. J.*, vol. 48, pp. 2103–2132, Sept. 1969.

# Millimeter-Wave Image-Guide Integrated Passive Devices

JEFFREY A. PAUL AND YU-WEN CHANG, MEMBER, IEEE

**Abstract**—Millimeter-wave boron-nitride image-guide integrated passive devices such as couplers, detectors, and balanced mixers have been developed with performances comparable to their metal waveguide circuit counterparts.

#### I. INTRODUCTION

THE DIELECTRIC image guide, formed by placing the half-height rectangular cross-sectional dielectric guide on the metal plane, exhibits low propagation loss at millimeter-wave frequencies. Directional couplers, electronic phase shifters, filters, and active and passive devices of image-guide integrated circuit forms have been recently developed [1]–[4].

Complex millimeter-wave integrated circuit structures can be easily formed from dielectric materials using sandblasting, machining, laser cutting techniques, and

even casting. They are a low-cost approach to millimeter-wave circuits compared to metal waveguide circuits which require precision machining, especially at frequencies beyond 60 GHz.

Boron nitride has been used successfully by us as the image-guide material for both active and passive circuit integration [1]. This paper reports our results on the loss characteristics of the boron-nitride material and on the boron-nitride image-guide integrated circuits (BNIGIC) passive devices such as couplers, detectors, and balanced mixers for use in communications and radar systems.

#### II. BORON-NITRIDE IMAGE-GUIDE CHARACTERISTICS

Boron nitride (BN) has a dielectric constant between 4.10 and 3.97, depending on the direction of pressing as measured by us at 53.84 GHz. Dielectric loss of the material in the millimeter-wave frequency spectrum was determined by measuring the line loss of a 2-in section of a dielectric waveguide made of BN. Fig. 1 shows the

Manuscript received November 1, 1977. This work was supported by the U.S. Army Electronics Research and Development Command, Fort Monmouth, NJ, under Contracts DAAB07-76-C-1353 and DAAB07-76-C-A101.

The authors are with the Electron Dynamics Division, Hughes Aircraft Company, Torrance, CA 90509.